Scientific Note

Study of black holes with the ATLAS detector at the LHC

J. Tanaka[1,a], T. Yamamura[2], S. Asai[1], J. Kanzaki[3]

[1] International Center for Elementary Particle Physics (ICEPP), University of Tokyo, 7-3-1 Hongo, Bunkyo-ku, Tokyo, 113-0033, Japan
[2] Department of Physics, Faculty of Science, University of Tokyo, 7-3-1 Hongo, Bunkyo-ku, Tokyo, 113-0033, Japan
[3] High Energy Accelerator Research Organization (KEK), IPNS, 1-1 Oho, Tsukuba, Ibaraki, 305-0801, Japan

Abstract. We evaluate the potential of the ATLAS detector for discovering black holes produced at the LHC, as predicted in models with large extra dimensions where quantum gravity is at the TeV scale. We assume that black holes decay by Hawking evaporation to all Standard Model particles democratically. We comment on the possibility to estimate the Planck scale.

1 Introduction

Black holes (BHs) will be produced at the Large Hadron Collider (LHC) if the fundamental Planck scale is of order a TeV [1,2]. This scenario occurs in the model of large extra dimensions [3] proposed by Arkani-Hamed, Dimopoulos and Dvali, where the Standard Model (SM) gauge and matter fields are confined to a 3-dimensional brane while gravity is free to propagate in extra dimensions of large size. This model was motivated by the desire to solve the hierarchy problem.

Using Gauss' law, the fundamental Planck scale of the $(4+n)$-dimension M_P is related to the 4-dimensional Planck scale $M_{\rm Pl}$ ($\sim 10^{19}$ GeV) by

$$M_{\rm Pl}^2 \sim M_P^{n+2} R^n,$$

where n is the number of extra dimensions and R is the size of the compactified dimensions. Assuming that the fundamental Planck scale M_P is the same as the electroweak scale ($\sim$1 TeV), the case $n = 1$ yields a very large R ($\sim 10^{13}$ cm), ruled out by experiments. For $n \geq 2$, the size of R is less than $\sim 10^{-2}$ cm, which does not contradict results of gravitational experiments [4]. From astrophysical constraints [5], the size of M_P is larger than $O({\rm TeV})$ and $O(10\ {\rm TeV})$ for $n = 2$ and 3, respectively. In particular, the case of $n = 2$ would be ruled out from the point of view of the solution of the hierarchy problem [6].

We consider here black holes of mass $M_{\rm BH}$ much larger than the fundamental Planck scale M_P since the phenomenology of black holes at $M_{\rm BH} \sim M_P$ is very complex and beyond the scope of the present study.

[a] e-mail: Junichi.Tanaka@cern.ch

For the collision of two partons at a center-of-mass energy $\sqrt{\hat{s}} = M_{\rm BH}$, by classical arguments [1] the total cross section is given by

$$\sigma(M_{\rm BH}) \sim \pi R_{\rm S}^2 = \frac{1}{M_P^2} \left[\frac{M_{\rm BH}}{M_P} \left(\frac{8\Gamma(\frac{n+3}{2})}{n+2} \right) \right]^{\frac{2}{1+n}},$$

where $R_{\rm S}$ is the Schwarzschild radius:

$$R_{\rm S} = \frac{1}{\sqrt{\pi}M_P} \left[\frac{M_{\rm BH}}{M_P} \left(\frac{8\Gamma(\frac{n+3}{2})}{n+2} \right) \right]^{\frac{1}{1+n}}.$$

For proton-proton collisions at the LHC, the differential cross section is given by

$$\frac{d\sigma(pp \to {\rm BH} + X)}{dM_{\rm BH}} = \frac{dL}{dM_{\rm BH}} \hat{\sigma}(ab \to {\rm BH})|_{\hat{s}=M_{\rm BH}^2}, \quad (1)$$

$$\frac{dL}{dM_{\rm BH}} = \frac{2M_{\rm BH}}{s} \sum_{a,b} \int_{M_{\rm BH}^2/s}^1 \frac{dx_a}{x_a} f_a(x_a) f_b\left(\frac{M_{\rm BH}^2}{s x_a} \right)$$

$$\hat{\sigma}(ab \to {\rm BH})|_{\hat{s}=M_{\rm BH}^2} = \pi R_{\rm S}^2,$$

where a and b are partons in protons and $f_i(x)$ are the parton distribution functions (PDFs). An exponential suppression of the geometrical cross section has been proposed by Voloshin [7]. However since subsequent studies did not support this result [8], we do not consider the effect here.

Black holes decay through several phases [2]: *balding*, *Hawking evaporation* (*spin-down* and *Schwarzschild*) and *Planck* phases. Since the *Hawking evaporation* phase is expected to be the main phase of the decay, we naively consider only this process and assume that a black hole evaporates until its mass becomes zero.

The radiation is characterized by the Hawking temperature T_H,

$$T_H(M_P, n, M_{\mathrm{BH}}) = M_P \left(\frac{M_P}{M_{\mathrm{BH}}} \frac{n+2}{8\Gamma(\frac{n+3}{2})} \right)^{\frac{1}{n+1}} \frac{n+1}{4\sqrt{\pi}}$$

$$= \frac{n+1}{4\pi R_{\mathrm{S}}} .$$

The heavier the black hole, the colder are its decay products. As it evaporates, its temperature increases but we will ignore the time evolution of black holes in this phase.

We assume that the evaporation is described by black body radiation. The energy spectrum of the decay products obeys the Boltzmann distribution [1]:

$$\frac{dN}{dE} \sim \frac{x^2}{e^x + c} ,$$

where $x \equiv E/T_H$ and c is a constant, which depends on the quantum statistics of the decay products, i.e., $c = -1, +1, 0$ for bosons, fermions and Boltzmann statistics, respectively. In this study, we use $c = 0$ for all particles.

Certain conservation laws are obeyed in the decay of black holes. We assume that black holes decay "democratically", i.e., with roughly equal probability to all of the SM particles.

In this paper, we present the discovery potential for black holes at the LHC. We describe a method of estimation of the fundamental Planck scale M_P from the discovery potential.

The outline of this paper is as follows: the simulation conditions and description of signal and background samples are given in Sect. 2. Our original generator of the black holes is explained in detail in Sect. 3. In Sect. 4, we describe the event selection and the reconstruction and finally, a conclusion is given in Sect. 5.

2 Simulation

The generator, developed for the purpose of this study, is described in Sect. 3. Initial state parton showers, hadronisation and decay are performed using PYTHIA 6.2 [9]. All background samples are generated by PYTHIA 6.2. CTEQ5L is used for the parton distribution function.

All samples are processed through the parameterized simulator, ATLFAST [10], of the ATLAS detector. The energy resolutions and efficiencies for jet and particle reconstruction are corrected using the results of the full detector simulation.

2.1 Signal

We have generated signal samples for the various values of (M_P, n) listed in Table 1. We have generated black holes whose mass M_{BH} is larger than M_P. Factorization and renormalization scales are set to the mass M_{BH} of the generated black hole. We call the lower limit of a black hole mass a threshold mass $M_{\mathrm{BH}}^{\mathrm{th}} = f_{\mathrm{BH}}^{\mathrm{th}} \times M_P$. We assume that the energy spectrum of all the products from the black hole decay obeys the Boltzmann distribution.

Table 1. Cross section of signal samples for each (M_P, n) parameter. $f_{\mathrm{BH}}^{\mathrm{th}}$, which is described in the text, is 1 for all cases. The unit of M_P is TeV

M_P, n	σ (pb)	M_P, n	σ (pb)
1,2	$9.45 \cdot 10^3$	5,2	0.662
1,3	$8.26 \cdot 10^3$	5,3	0.603
1,4	$8.06 \cdot 10^3$	5,5	0.625
1,5	$8.24 \cdot 10^3$	5,7	0.699
1,7	$9.05 \cdot 10^3$		
3,2	25.5	6,2	0.125
3,3	22.9	6,3	0.114
3,5	23.4	6,5	0.119
3,7	26.0	6,7	0.133
4,2	3.74	7,2	0.0229
4,3	3.38	7,3	0.0210
4,5	3.49	7,5	0.0220
4,7	3.89	7,7	0.0247

Table 2. Cross section of background samples for each mode. "Proc" is a process identification defined in PYTHIA

Process	σ (pb)	$\hat{p}_T^{min}$	Proc
qq (q =quark,	$1.29 \cdot 10^4$	280.0	11,12,13,
lepton,gluon)			28,53,68
$t\bar{t}$	493	10.0	81,82
$W^{\pm}W^{\mp}$	0.468	240.0	25
$W^{\pm}Z$	25.9	10.0	23
ZZ	10.6	10.0	22
$\gamma\gamma$	229	10.0	18,114
γV ($V = W^{\pm}, \gamma^*, Z$)	280	10.0	19,20
$W^{\pm}q$	73.4	240.0	16,31
$Zq, \gamma^* q$	31.5	240.0	15,30
γq	23.5	240.0	14,29,115

2.2 Background

Our background samples are listed in Table 2. We use kinematical cuts at generation level to save CPU time and storage space of the data. The lower limit for the energy in the center-of-mass of initial partons is set to 50 GeV for all the samples. The lower limit for the transverse momentum in the rest frame of initial partons, $\hat{p}_T^{min}$, is also used as shown in Table 2.

3 Generator

A black hole generator was developed for this study, based on the assumptions and approximations discussed in Sect. 1[1]. It is appropriate to use simple assumptions for

---

[1] Assumptions and approximations of our generator are similar to those of the generator TRUENOIR described in [11]. Another generator has been published [12].

the production and decay of black holes in order to study mainly the discovery potential at the LHC.

We require the following conditions for the decay of black holes:

- Constraint of the number of fermions by spin conservation
- Four-Momentum conservation
- Assumption of Boltzmann distribution for the energy spectrum of decay products
- Color conservation
- Assumption of democratic decay
- Charge conservation
- Option of conservation of the difference between the lepton number and the baryon number ($B - L$ conservation)
- Option of implementing Voloshin suppression [7]

We can select whether to apply the $B-L$ conservation and the Voloshin suppression, but they are switched off (no $B - L$ conservation and no Voloshin suppression) in this study.

For the production of the black holes, we use (1) of Sect. 1. Using the PDFs, the types of partons in the initial hard scattering are selected randomly.

3.1 Spin conservation

We require that the number of fermions in the decay products of the black holes be even or odd according to the parity of the number of initial state fermions. Note that we do not consider gravitons in this study.

3.2 Four-momentum conservation and Boltzmann distribution

We assume that the energy spectrum of the decay products follows a Boltzmann distribution. However, since energy and momentum must be conserved, not all particles can be sampled randomly from that distribution. We do not allow the case $N = 2$ since it is fully constrained. For $N \geq 3$, particle energies are successively sampled from the Boltzmann distribution until the summed energy exceeds the mass of the black hole. The last particle is then given the energy required by the energy constraint. The first $N - 2$ particles are assigned random directions and the last two are emitted in a direction such as to conserve overall momentum.

3.3 Color conservation

Color is assumed to be conserved in the decay of black holes. Color is assigned to the initial partons and color connection is implemented. As an example, if the initial partons are two gluons, we select randomly either a $q\bar{q}$ pair or a gluon from the final state partons, if present. We then connect the colors as shown in Fig. 1. If no $q\bar{q}$ pair or gluon is present, the color connection must be applied
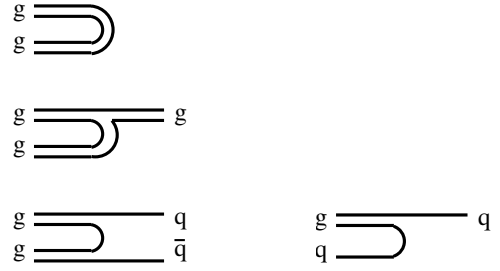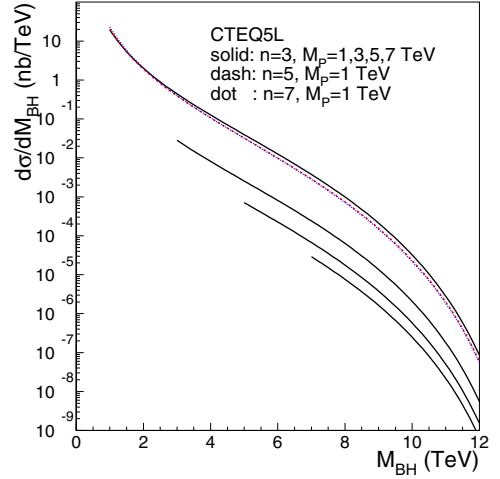

Fig. 1. Color connection for gg (left) and gq (right)

Fig. 2. Differential cross section as a function of black hole mass for each (M_P,n) parameter

Table 3. Degrees of freedom and assigned probability in the generator for each particle

Particle	Degrees of freedom	Assigned probability
g (gluon)	8	0.0690
W	6	0.0517
Z	3	0.0259
γ	2	0.0172
lepton (e, μ, τ)	4	0.0345
neutrino $(\nu_e, \nu_\mu, \nu_\tau)$	4	0.0345
quark (u, d, c, s, t, b)	12	0.1034
Higgs	1	0.0086
Graviton	5	0.0000

between the two initial state gluons, if possible. Another example of color connection when the initial partons are a quark and a gluon is shown in Fig. 1.

For the remaining partons, color connection is applied between pairs with closest opening angle. If there is an odd gluon remaining, it is connected to the $q\bar{q}$ pair or a gg pairs or to the initial partons.

a $(M_P, n)=(1,3)$

b $(M_P, n)=(1,7)$

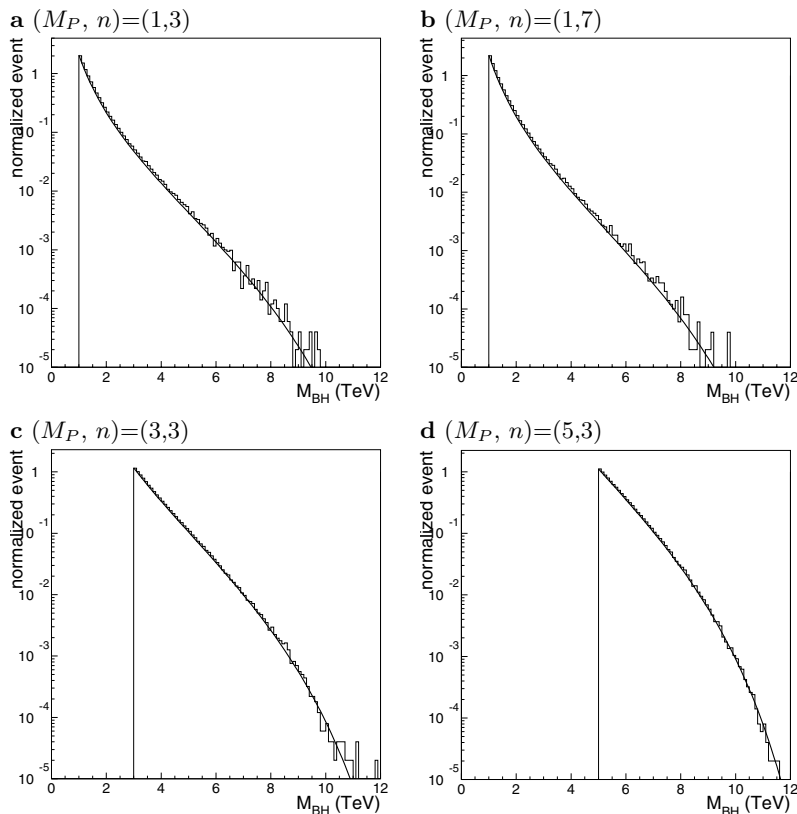**c** $(M_P, n)=(3,3)$

d $(M_P, n)=(5,3)$

Fig. 3. Mass distributions of the generated black holes. The histogram shows generated black holes and the solid line shows an expected shape from (1)

3.4 Democratic decay

We assume a democratic decay, constrained by the conservation laws. The number of degrees of freedom for each particle takes into account charge, spin and color. We do not consider gravitons in this study. The mass of the SM Higgs is set at 120 GeV. Events are produced in which the types of particles are chosen randomly with the probabilities listed in Table 3 and are accepted only if conservation laws can be applied.

3.5 Performance

Figure 2 shows the differential cross sections, calculated from (1). Figures 3 show the shape of the mass distributions of generated black holes. The distributions shown start at $M_{BH} > M_P$ although, as mentioned above, the validity of the model applies in the region $M_{BH} \gg M_P$.

Figures 4 show various distributions of the generated black holes: p_z, charge, lepton number (L), baryon number (B), $B - L$, and the multiplicity of decay products. The absolute values of L are always even because of spin conservation as shown at Figs. 4 (c) and (g). When spin conservation is turned off, they take on both even and odd values, as shown at Figs. 4 (h). Figures 4 (f),(i) and (j) indicate that the multiplicity of decay products depends on M_{BH} not M_P.

The distribution of particle types in the decay of black holes are shown in Figs. 5. As expected, there are more quarks than anti-quarks (Figs. 5a and b) since the LHC

is a proton-proton collider. We have also generated signal samples with $(M_P, n, f_{BH}^{th})=(1,3,9)$ in order to analyze events with high multiplicity of decay products. As the multiplicity of decay products becomes larger, the proportion of each product becomes closer to the values of Table 3, even when many conservations are imposed, as can be seen in Figs. 5 (c) and (d). When there is no charge and spin conservation, the ratios are almost the same as the values of Table 3, as shown at Figs. 5 (e) and (f).

Figures 6 show various distributions of the decay products: p_T, p_z, energy, η and ϕ. Distributions of p_z, η and ϕ of the products are symmetric as expected. Note that we have generated 10^5 events at each point (Figs. 4, 5 and 6).

4 Analysis

Although the expressions for black hole production given in Sect. 1 are not valid at $M_{BH} \sim M_P$, our BH generator applies them in all the regions where $M_{BH} > M_P$ in this study.

4.1 Selection criteria and reconstruction

The following cuts are applied in order to select and reconstruct black holes:

– For a precise reconstruction of the BH, it is necessary to remove particles produced in the stage of initial state radiation (ISR). Because the particles from
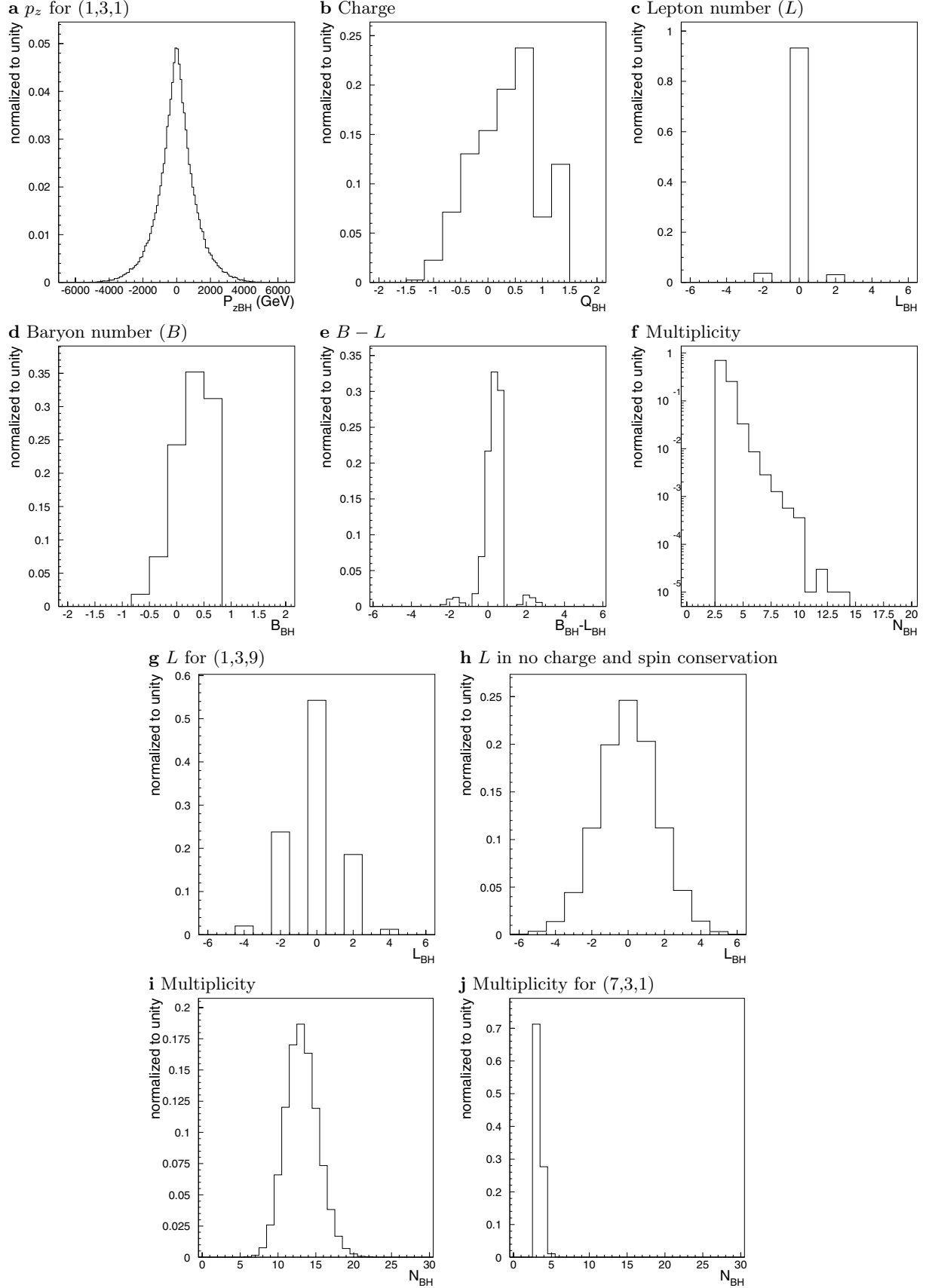
Fig. 4. Distributions of generated black hole properties: p_z, charge, lepton number (L), baryon number (B), $B - L$, and multiplicity of decay products. **a**–**f** for $(M_P, n, f_{\mathrm{BH}}^{\mathrm{th}})=(1,3,1)$, **g**–**i** for $(M_P, n, f_{\mathrm{BH}}^{\mathrm{th}})=(1,3,9)$ and **j** for $(M_P, n, f_{\mathrm{BH}}^{\mathrm{th}})=(7,3,1)$

a PDG code for (1,3,1)

b |PDG code| for (1,3,1)

c PDG code for (1,3,9)

d |PDG code| for (1,3,9)

e PDG code for (1,3,9)
in no charge and spin conservation.

f |PDG code| for (1,3,9)
in no charge and spin conservation
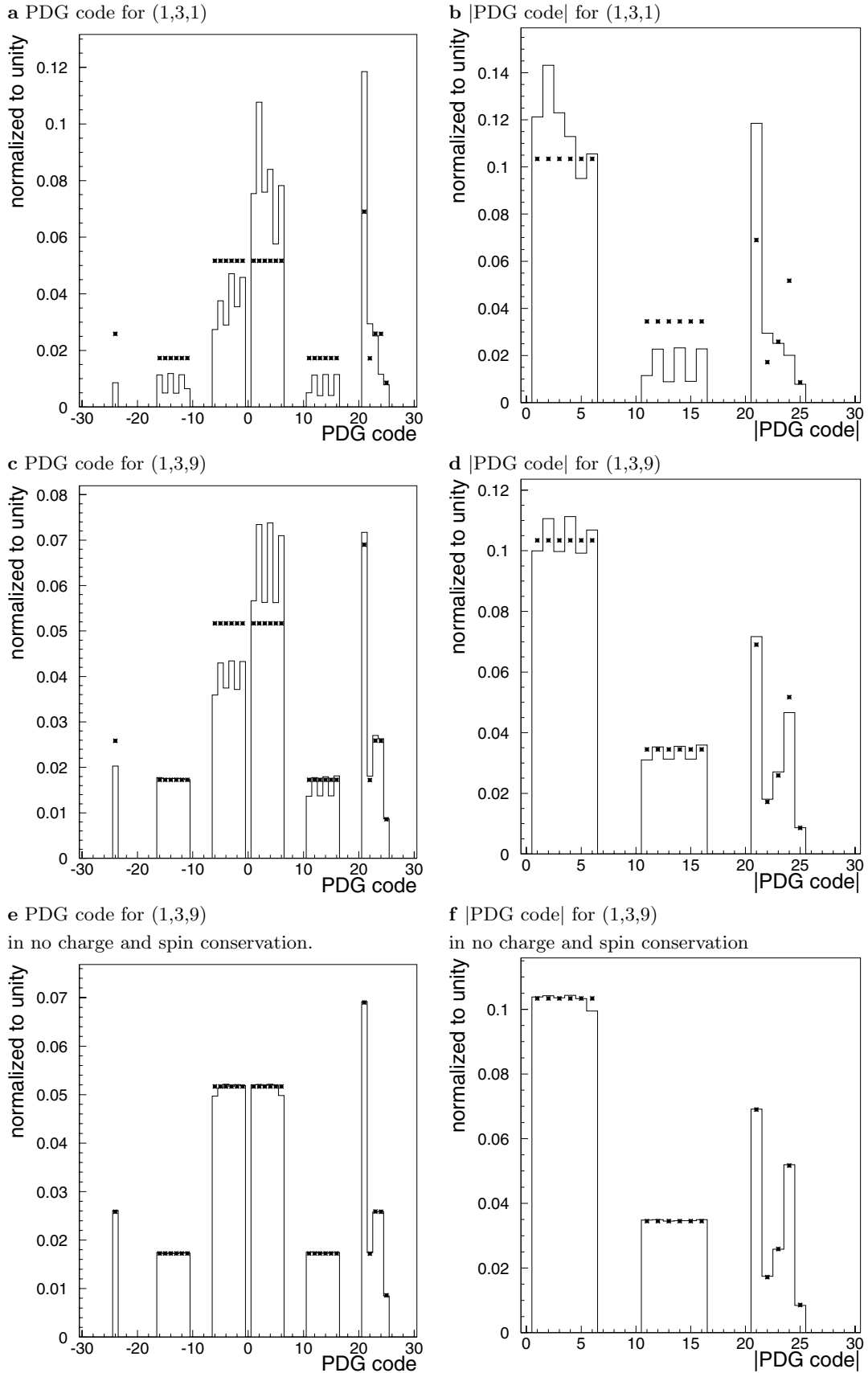
Fig. 5. Distributions of PDG code of decay products of black holes for different cases of $(M_P, n, f_{\mathrm{BH}}^{\mathrm{th}})$. The left shows PDG code and the right shows the absolute value of PDG code. The points of * show the values at Table 3

Fig. 6. Distributions of various properties of decay products of black holes: p_T, p_z, energy, η and ϕ. **a–e** for $(M_P, n, f_{\rm BH}^{\rm th}) = (1,3,1)$, **fg** for $(M_P, n, f_{\rm BH}^{\rm th}) = (1,3,9)$ and **hi** for $(M_P, n, f_{\rm BH}^{\rm th}) = (7,3,1)$

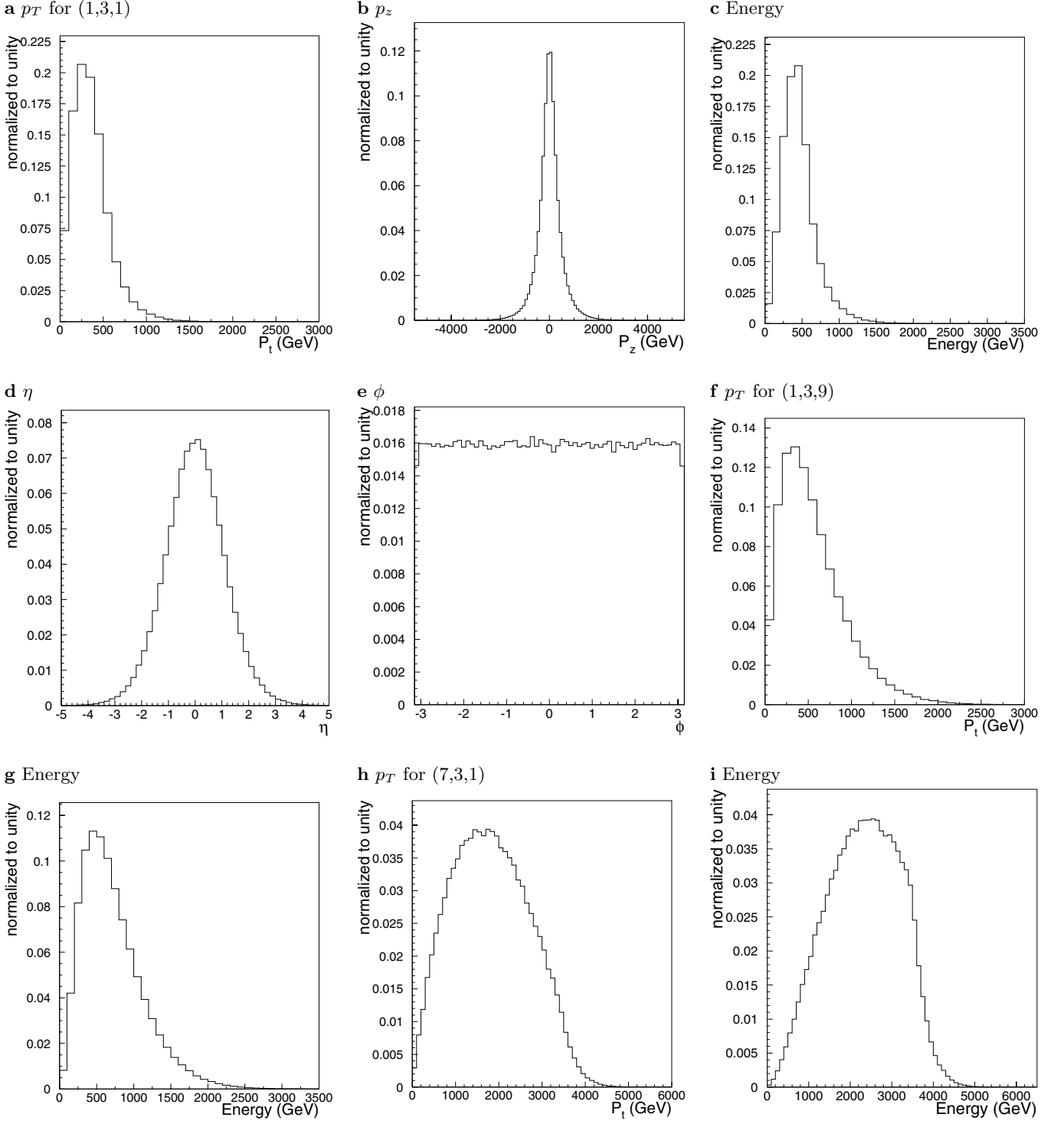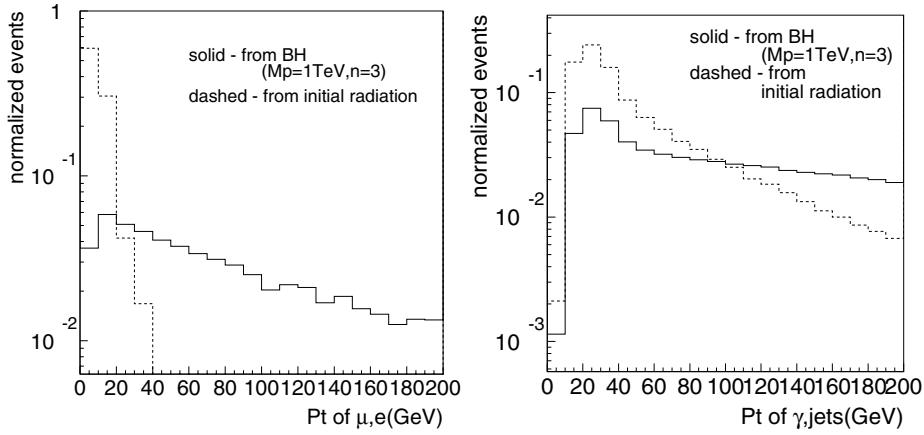**Fig. 7.** p_T distributions : comparison between particles from BH and initial state radiation ($M_P = 1$ TeV, $n=3$)

ISR tend to have small p_T and large $|\eta|$, as shown in Figs. 7 and 8, the following requirements are applied to particles in each event (ISR-cut) :

- $p_T > 30$ GeV   for μ, e
- $p_T > 50$ GeV   for γ, jet

- Of all the particles passing the ISR-cut, more than three are required to have energy larger than 300 GeV ($E > 300$ GeV), and moreover, at least one of them has to be either an electron or a photon. This latter requirement is to suppress backgrounds. Figure 9 shows the distributions of the number of energetic particles in each event, where γq event is one of the largest contribution in the backgrounds as shown in Table 4. It is seen that this multiplicity cut on energetic particles is very effective.

- We require the event shape variable R_2 to be less than 0.8 ($R_2 < 0.8$). R_2 represents an event topology and it is defined by Fox-Wolfram moments as follows:

$$R_2 \equiv H_2/H_0$$

$$H_i \equiv \sum_{j,k} \frac{|p_j^*||p_k^*|}{E^2} P_i(\cos\phi_{jk})$$

where H_i is the i-th Fox-Wolfram moments, j and k are ID numbers of tracks, p_j^* is the momentum of the track j in the rest frame of BH, ϕ_{jk} is the opening angle between the tracks j and k , and $P_i(x)$ is the Legendre polynomial. E is obtained by summing up the energies of particles passing the ISR-cut, calculated in the rest frame of BH. R_2 ranges from 0 to 1 ($0 \leq R_2 \leq 1$) as can be seen from Fig. 10 which shows the R_2 distribution for signal and qq events with or without selection criteria. Since lower value of R_2 indicates more spherical event, we remove qq events here.

- $E\!\!\!/_T < 100$ GeV. For a precise calculation of BH mass, events with high missing energy are rejected here.

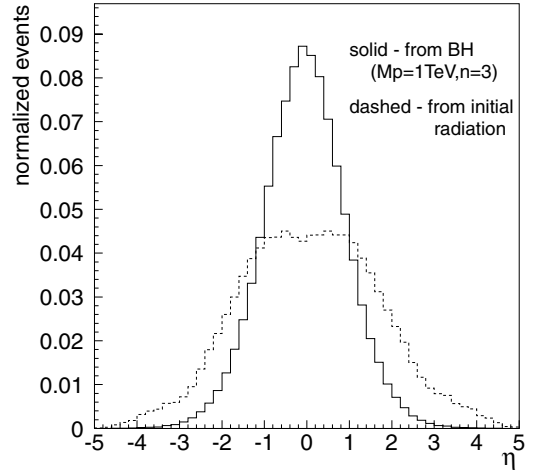**Fig. 8.** η distributions : comparison between particles from BH and initial state radiation ($M_P = 1$ TeV, $n=3$)
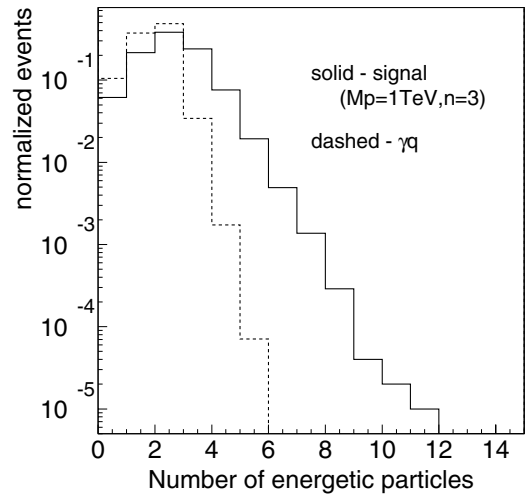

Fig. 9. Shape of the distribution of the number of energetic particles with $E > 300$ GeV : comparison between signal and γq background ($M_P = 1$ TeV, $n=3$)
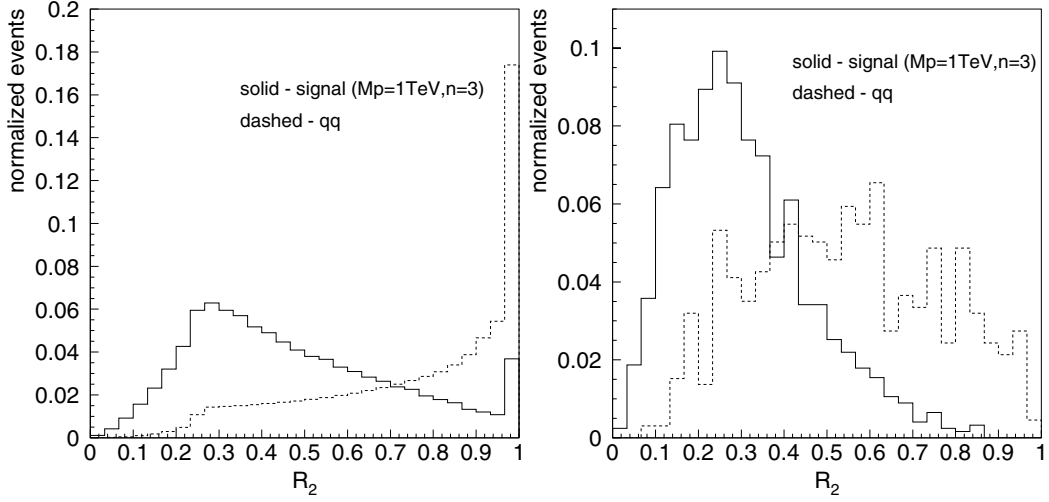
Fig. 10. R_2 Distributions : comparison between signal event and qq event ($M_P = 1$ TeV, $n=3$). Left: without any selection criteria and right: with selection criteria

Table 4. The number of remaining BG events at $\int \mathcal{L}dt = 10$ fb^{-1}. $\varepsilon^{M_{\mathrm{BH}}^{\min}=1}$ is the value of efficiency for $M_{\mathrm{BH}}^{\min} = 1$ TeV

		qq	$t\bar{t}$	$W^\pm W^\mp$
σ (pb)		$1.29\cdot10^4$	493	0.468
$\varepsilon^{M_{\mathrm{BH}}^{\min}=1}$		$1.67\cdot10^{-5}$	$1.39\cdot10^{-5}$	$8.5\cdot10^{-5}$
	1.0	$2.15\cdot10^3$	68.5	0.40
$M_{\mathrm{BH}}^{\min}$	2.0	$1.18\cdot10^3$	13	0.1
	3.0	$4.3\cdot10^2$	2	0.02
(TeV)	4.0	77	0.5	0
	5.0	$3\cdot10$	0	0

		$W^\pm Z$	ZZ	$\gamma\gamma$	γV
σ (pb)		25.9	10.6	229	280
$\varepsilon^{M_{\mathrm{BH}}^{\min}=1}$		$5\cdot10^{-7}$	$1.5\cdot10^{-6}$	0	$7\cdot10^{-7}$
	1.0	0.1	0.084	0	2
$M_{\mathrm{BH}}^{\min}$	2.0	0.05	0.04	0	1
	3.0	0	0	0	0
(TeV)	4.0	0	0	0	0
	5.0	0	0	0	0

		$W^\pm q$	Zq,γ^*q	γq	total
σ (pb)		73.4	31.5	23.5	
$\varepsilon^{M_{\mathrm{BH}}^{\min}=1}$		$4.7\cdot10^{-5}$	$1.40\cdot10^{-4}$	$1.484\cdot10^{-3}$	
	1.0	35	44.2	349.3	$2.66\cdot10^3$
$M_{\mathrm{BH}}^{\min}$	2.0	18	21	195	$1.43\cdot10^3$
	3.0	4	3.5	49.2	$4.9\cdot10^2$
(TeV)	4.0	0.7	0.3	7.8	86
	5.0	0	0	2.8	$3\cdot10$

The black hole mass is then reconstructed from the 4-momenta of the remaining muons, electrons, gammas and jets as follows:

$$p_{\mathrm{BH}} = \sum_{i=\mu,e,\gamma,jet} p_i$$

$$M_{\mathrm{BH}} = \sqrt{p_{\mathrm{BH}}^2},$$

where p_i is a reconstructed four-momentum of each particle.

The quality of the reconstructed mass of the BH is discussed in Appendix A.

4.2 Discovery potential

We have evaluated the discovery potential for the following cases of (M_P, n):

$$\begin{cases} M_P = 1, 3, 4, 5, 6, 7 \text{ TeV} \\ n = 2, 3, 5, 7 \end{cases}$$

by using the selection criteria described in Sect. 4.1. Because M_P is an unknown parameter, we cannot set the proper cut value for the lower limit of the reconstructed M_{BH}. Therefore we consider various values as follows and evaluate $S/\sqrt{B}$ in each case:

$$M_{\mathrm{BH}} > M_{\mathrm{BH}}^{\min} = 1, 2, 3, 4, 5 \text{ TeV}.$$

The M_{BH} distributions are shown in Fig. 11 for different values of M_P with $n = 3$. These are obtained after all the selection criteria have been applied. The histograms represent the sum of signals and backgrounds with the cross-hatched part showing only backgrounds. Note that $M_{\mathrm{BH}}^{\min}$ is set to 1 TeV for this figure.

Tables 4–6 show the number of events passing the selection criteria for background (BG) processes and signal events with various (M_P, n). The number is normalized for $\int \mathcal{L}dt = 10$ fb^{-1}. The values of efficiency are listed only for $M_{\mathrm{BH}}^{\min} = 1$ TeV. As can be seen in Table 4, γq process

a M_P=1 TeV

b M_P=3 TeV

c M_P=4 TeV

d M_P=5 TeV

e M_P=6 TeV

f M_P=7 TeV

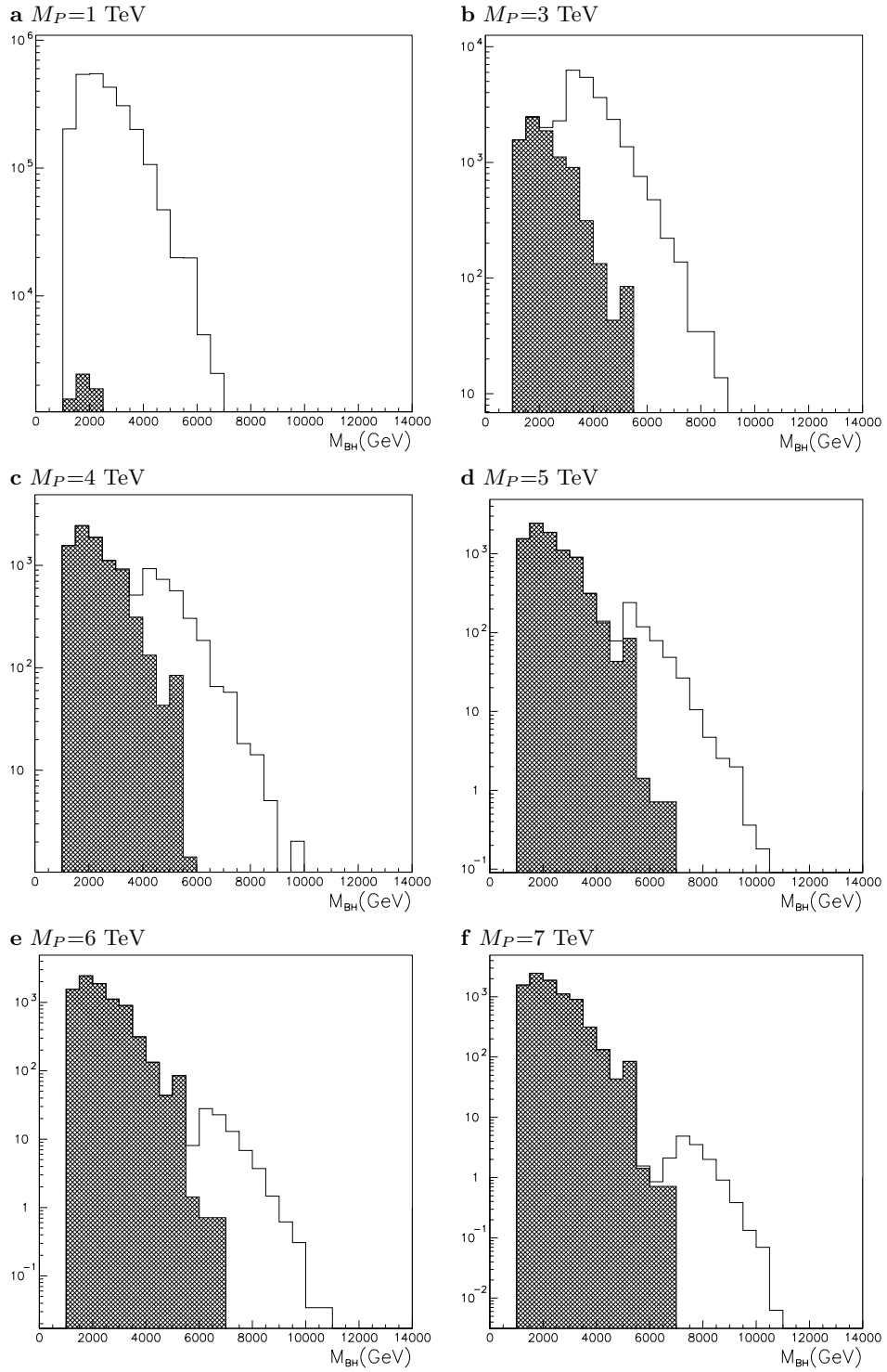**Fig. 11.** M_{BH} distributions in the case of n=3 and $M_{\mathrm{BH}}^{\mathrm{min}}$=1 TeV. (solid line : signal plus background, cross hatched : background only)

Table 5. The number of remaining signal events at $\int \mathcal{L}dt$=10 fb^{-1}. $\varepsilon^{M_{\mathrm{BH}}^{\mathrm{min}}=1}$ is the value of efficiency for $M_{\mathrm{BH}}^{\mathrm{min}} = 1$ TeV

(M_P, n)		(1,2)	(3,2)	(4,2)
σ (pb)		9450	25.51	3.738
$\varepsilon^{M_{\mathrm{BH}}^{\mathrm{min}}=1}$			9.63×10^{-3}	2.747×10^{-2}	2.733×10^{-2}
	1.0	9.10×10^5	7008	1022
$M_{\mathrm{BH}}^{\mathrm{min}}$	2.0	6.50×10^5	7002	1021
	3.0	2.52×10^5	6594	1016
(TeV)	4.0	7.5×10^4	2987	943.5
	5.0	2.3×10^4	1.06×10^3	404.5

(M_P, n)		(5,2)	(6,2)	(7,2)
σ (pb)		0.6622	0.1249	2.292×10^{-2}
$\varepsilon^{M_{\mathrm{BH}}^{\mathrm{min}}=1}$		2.601×10^{-2}	2.287×10^{-2}	2.022×10^{-2}
	1.0	172.2	28.56	4.634
$M_{\mathrm{BH}}^{\mathrm{min}}$	2.0	172.2	28.54	4.634
	3.0	171.7	28.53	4.632
(TeV)	4.0	170.1	28.46	4.616
	5.0	154.2	28.15	4.593

(M_P, n)		(1,3)	(3,3)	(4,3)
σ (pb)		8256	22.89	3.381
$\varepsilon^{M_{\mathrm{BH}}^{\mathrm{min}}=1}$		8.46×10^{-3}	2.725×10^{-2}	2.605×10^{-2}
	1.0	6.98×10^5	6238	880.8
$M_{\mathrm{BH}}^{\mathrm{min}}$	2.0	4.82×10^5	6224	879.4
	3.0	2.01×10^5	5878	874.0
(TeV)	4.0	5.8×10^4	2745	810.8
	5.0	1.2×10^4	929	354.3

(M_P, n)		(5,3)	(6,3)	(7,3)
σ (pb)		0.6027	0.1142	2.105×10^{-2}
$\varepsilon^{M_{\mathrm{BH}}^{\mathrm{min}}=1}$		2.574×10^{-2}	2.347×10^{-2}	2.071×10^{-2}
	1.0	155.1	26.80	4.359
$M_{\mathrm{BH}}^{\mathrm{min}}$	2.0	155.1	26.80	4.357
	3.0	154.4	26.76	4.351
(TeV)	4.0	152.7	26.59	4.341
	5.0	140.4	26.23	4.317

Table 6. The number of remaining signal events at $\int \mathcal{L}dt$=10 fb^{-1}. $\varepsilon^{M_{\mathrm{BH}}^{\mathrm{min}}=1}$ is the value of efficiency for $M_{\mathrm{BH}}^{\mathrm{min}} = 1$ TeV

(M_P, n)		(1,5)	(3,5)	(4,5)
σ (pb)		8244	23.42	3.487
$\varepsilon^{M_{\mathrm{BH}}^{\mathrm{min}}=1}$		7.24×10^{-3}	2.563×10^{-2}	2.779×10^{-2}
	1.0	5.97×10^5	6003	969.0
$M_{\mathrm{BH}}^{\mathrm{min}}$	2.0	4.24×10^5	5993	969.0
	3.0	1.72×10^5	5600	964.5
(TeV)	4.0	5.0×10^4	2497	892.0
	5.0	1.4×10^4	775	377.3

(M_P, n)		(5,5)	(6,5)	(7,5)
σ (pb)		0.6252	0.1191	2.203×10^{-2}
$\varepsilon^{M_{\mathrm{BH}}^{\mathrm{min}}=1}$		2.501×10^{-2}	2.244×10^{-2}	2.139×10^{-2}
	1.0	156.4	26.73	4.712
$M_{\mathrm{BH}}^{\mathrm{min}}$	2.0	156.3	26.73	4.712
	3.0	155.7	26.69	4.706
(TeV)	4.0	154.9	26.61	4.688
	5.0	139.2	26.33	4.662

(M_P, n)		(1,7)	(3,7)	(4,7)
σ (pb)		9053	26.02	3.887
$\varepsilon^{M_{\mathrm{BH}}^{\mathrm{min}}=1}$		6.54×10^{-3}	2.577×10^{-2}	2.630×10^{-2}
	1.0	5.92×10^5	6705	1022
$M_{\mathrm{BH}}^{\mathrm{min}}$	2.0	4.22×10^5	6698	1020
	3.0	1.57×10^5	6310	1017
(TeV)	4.0	4.5×10^4	2789	943.0
	5.0	5×10^3	892	382

(M_P, n)		(5,7)	(6,7)	(7,7)
σ (pb)		0.6991	0.1335	2.474×10^{-2}
$\varepsilon^{M_{\mathrm{BH}}^{\mathrm{min}}=1}$		2.577×10^{-2}	2.319×10^{-2}	2.090×10^{-2}
	1.0	180.2	30.96	5.171
$M_{\mathrm{BH}}^{\mathrm{min}}$	2.0	180.2	30.93	5.171
	3.0	179.7	30.89	5.168
(TeV)	4.0	178.3	30.72	5.151
	5.0	164.7	30.48	5.124

has the highest efficiency, but the background is dominated by the qq process owing to its large cross section. The total number of BG events is found to be $\sim 10^3$–10^4 in the case of $M_{\mathrm{BH}}^{\mathrm{min}}$ = 1–2 TeV and ~ 10–10^2 in the case of $M_{\mathrm{BH}}^{\mathrm{min}}$ = 4–5 TeV.

According to Tables 5 and 6, the efficiency for signal events is $\sim 1\%$ in all cases of (M_P, n). It is relatively lower when M_P = 1 TeV or 7 TeV because signal events are more likely to be rejected by the $M_{\mathrm{BH}}^{\mathrm{min}}$ cut in the case of smaller M_P, or they have a large $E\!\!\!/_T$ for larger M_P.

We calculate $S/\sqrt{B}$ from the data of Tables 4– 6 and estimate $\int \mathcal{L}_{\mathrm{discovery}}dt$– the integrated luminosity with which discovery is achieved. Here the condition of discov-ery is set as:

$$S/\sqrt{B} \geq 5.0 \qquad \text{and} \qquad S \geq 10$$

which is a conventional condition, as used in the analysis of Higgs events with ATLAS. The results for $S/\sqrt{B}$ and $\int \mathcal{L}_{\mathrm{discovery}}dt$ are shown in Table 7–8 and 9 respectively. We require that $M_{\mathrm{BH}}^{\mathrm{min}}$ be larger than M_P to calculate integrated luminosities for BH discovery. In Table 9, the shaded values indicate the most favorable cut in $M_{\mathrm{BH}}^{\mathrm{min}}$ in each case of (M_P, n). From these tables, we see that the discovery can be accomplished within $\int \mathcal{L}_{\mathrm{discovery}}dt \leq$ 1 fb^{-1} in all cases of n if M_P is less than ~ 5 TeV.

Table 7. The value of $S/\sqrt{B}$ at $\int \mathcal{L}dt$=10 fb^{-1}

(M_P,n)		(1,2)	(3,2)	(4,2)
σ (pb)		9450	25.51	3.738
	1.0	1.76×10^4	136	19.8
$M_{\mathrm{BH}}^{\min}$	2.0	1.72×10^4	185	27.0
	3.0	1.1×10^4	3.0×10^2	46
(TeV)	4.0	8.1×10^3	3.2×10^2	1.0×10^2
	5.0	4×10^3	2×10^2	7×10

(M_P,n)		(5,2)	(6,2)	(7,2)
σ (pb)		0.6622	0.1249	2.292×10^{-2}
	1.0	3.34	0.554	0.0899
$M_{\mathrm{BH}}^{\min}$	2.0	4.55	0.755	0.123
	3.0	7.8	1.3	0.21
(TeV)	4.0	18	3.1	0.50
	5.0	3×10	5	0.8

(M_P,n)		(1,3)	(3,3)	(4,3)
σ (pb)		8256	22.89	3.381
	1.0	1.35×10^4	121	17.1
$M_{\mathrm{BH}}^{\min}$	2.0	1.27×10^4	165	23.3
	3.0	9.1×10^3	2.7×10^2	39
(TeV)	4.0	6.3×10^3	3.0×10^2	87
	5.0	2×10^3	2×10^2	6×10

(M_P,n)		(5,3)	(6,3)	(7,3)
σ (pb)		0.6027	0.1142	2.105×10^{-2}
	1.0	3.01	0.520	0.0845
$M_{\mathrm{BH}}^{\min}$	2.0	4.10	0.709	0.115
	3.0	7.0	1.2	0.20
(TeV)	4.0	16	2.9	0.47
	5.0	3×10	5	0.8

Table 8. The value of $S/\sqrt{B}$ at $\int \mathcal{L}dt$=10 fb^{-1}

(M_P,n)		(1,5)	(3,5)	(4,5)
σ (pb)		8244	23.42	3.487
	1.0	1.16×10^4	116	18.8
$M_{\mathrm{BH}}^{\min}$	2.0	1.12×10^4	158	25.6
	3.0	7.8×10^3	2.5×10^2	44
(TeV)	4.0	5.4×10^3	2.7×10^2	96
	5.0	3×10^3	1×10^2	7×10

(M_P,n)		(5,5)	(6,5)	(7,5)
σ (pb)		0.6252	0.1191	2.203×10^{-2}
	1.0	3.03	0.518	0.0914
$M_{\mathrm{BH}}^{\min}$	2.0	4.13	0.707	0.125
	3.0	7.0	1.2	0.21
(TeV)	4.0	17	2.9	0.51
	5.0	3×10	5	0.9

(M_P,n)		(1,7)	(3,7)	(4,7)
σ (pb)		9053	26.02	3.887
	1.0	1.15×10^4	130	19.8
$M_{\mathrm{BH}}^{\min}$	2.0	1.11×10^4	177	27.0
	3.0	7.1×10^3	2.9×10^2	46
(TeV)	4.0	4.9×10^3	3.0×10^2	1.0×10^2
	5.0	9×10^2	2×10^2	7×10

(M_P,n)		(5,7)	(6,7)	(7,7)
σ (pb)		0.6991	0.1335	2.474×10^{-2}
	1.0	3.49	0.600	0.100
$M_{\mathrm{BH}}^{\min}$	2.0	4.77	0.818	0.137
	3.0	8.1	1.4	0.23
(TeV)	4.0	19	3.3	0.56
	5.0	3×10	6	0.9

Figure 12 gives a contour plot for $\int \mathcal{L}_{\mathrm{discovery}}dt$ in (M_P ,n) plane. We find that the discovery potential hardly depends on n but has a strong dependence on M_P. This is due to the fact that the cross section is a strong function of M_P but not of n, as shown in Tables 5 and 6. From this relation between M_P and $\int \mathcal{L}_{\mathrm{discovery}}dt$, M_P can be determined by how early the discovery is accomplished.

From a quantitative point of view, it is found that the excess of events is detected in ~ 1 month at low luminosity ($\int \mathcal{L}dt$=1 fb^{-1}) if $M_P < 5$ TeV, and discovery within only one day ($\int \mathcal{L}dt$=100 pb^{-1}) can be expected if $M_P < 4$ TeV.

As was previously mentioned, the BH model we assumed here is valid only when $M_{\mathrm{BH}} \gg M_P$. As M_{BH} approaches M_P, the theory of BH production becomes very complex. If we consider events with reconstructed $M_{\mathrm{BH}} > 5$ TeV in the case of $M_P = 1$ TeV, we find that we need ~ 5 pb^{-1} instead of ~ 0.1 pb^{-1} to discover black holes. However the events include black holes whose generated mass was less then 5 TeV. When black holes with mass greater than 5 TeV are generated, we find that we need ~ 10 pb^{-1}.

Considering that the model of BH formation and decay is valid only for $M_{\mathrm{BH}} \gg M_P$, we show, in Fig. 13, an evaluation of the discovery potential of BHs when the cut $M_{\mathrm{BH}}^{\min} > M_P + 1$ TeV is applied. Although more integrated luminosity is required, it is clear that an excess of events will still be easily observed within a few days of running, for M_P values up to a few TeV.

5 Conclusion

We have studied the potential to observe black holes with the ATLAS detector at the LHC. We developed a generator of black holes with simple assumptions for the production and decay process, taking the expressions in Sect. 1 as valid in the full region of the black hole mass $M_{\mathrm{BH}} > M_P$. We find an excess of events from the Standard Model backgrounds for the integrated luminosity of 1 fb^{-1} (~ 1 month at low luminosity) if $M_P < 5$ TeV and with the integrated
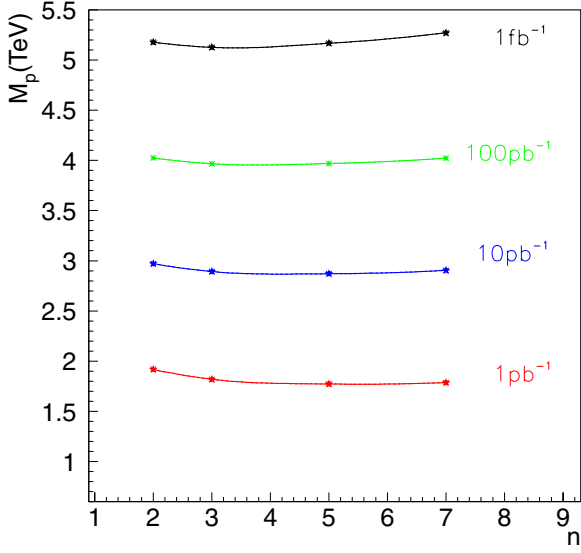
Fig. 12. Contours of $\int \mathcal{L}_{\text{discovery}} dt$ in (M_P, n) plane

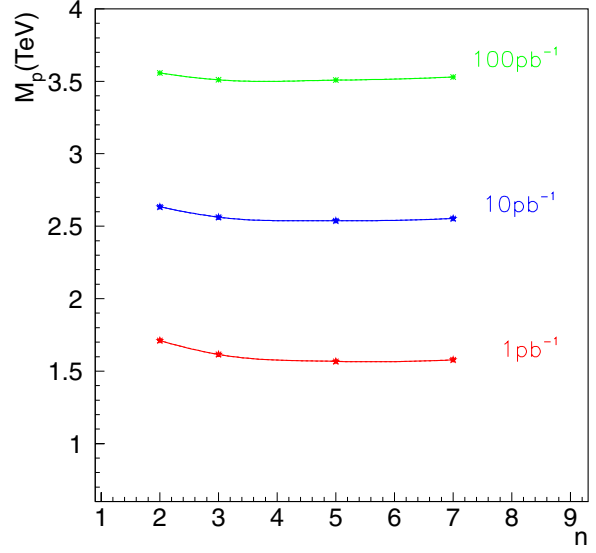**Fig. 13.** Contours of $\int \mathcal{L}_{\text{discovery}} dt$ in (M_P, n) plane in case of $M_{\text{BH}}^{\text{min}} > M_P + 1$ TeV
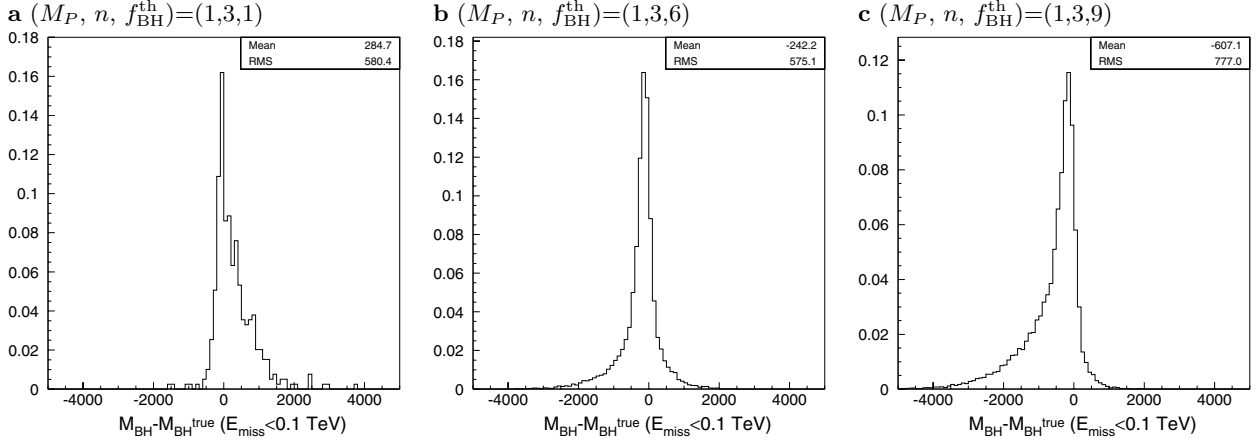

Fig. 14. Distributions of the difference between a reconstructed and a generated mass of a black hole $M_{\text{BH}} - M_{\text{BH}}^{\text{true}}$. Our selection criteria is applied to reconstruct a black hole. E_{miss} in the figure means $\not{E}_T$
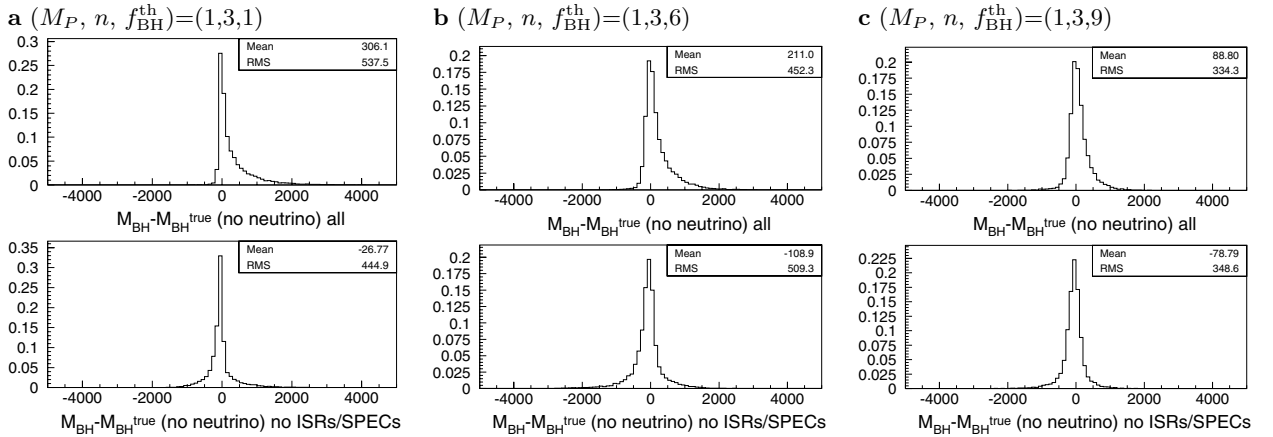

Fig. 15. $M_{\text{BH}} - M_{\text{BH}}^{\text{true}}$ Distributions. We use events with no neutrino. The upper figure is obtained from all reconstructed particles and jets and the lower is from them except for ISRs/SPECs. Details are given in the text
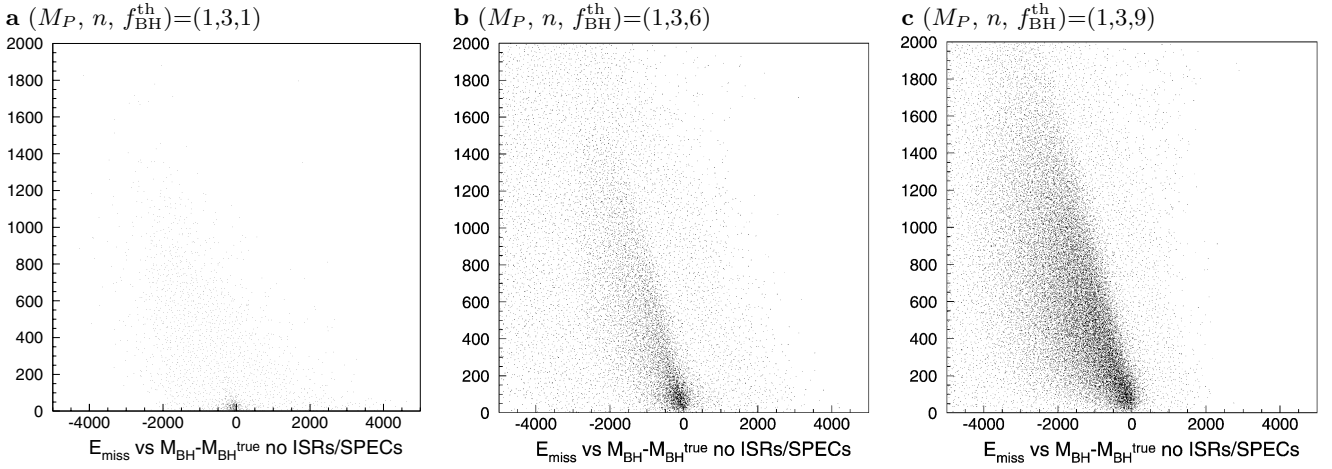
a $(M_P, n, f_{\mathrm{BH}}^{\mathrm{th}}) = (1,3,1)$ **b** $(M_P, n, f_{\mathrm{BH}}^{\mathrm{th}}) = (1,3,6)$ **c** $(M_P, n, f_{\mathrm{BH}}^{\mathrm{th}}) = (1,3,9)$

Fig. 16. Measured missing energy $E\!\!\!/_T$ versus $M_{\mathrm{BH}} - M_{\mathrm{BH}}^{\mathrm{true}}$. The mass of a black hole is obtained from reconstructed particles and jets except for ISRs/SPECs
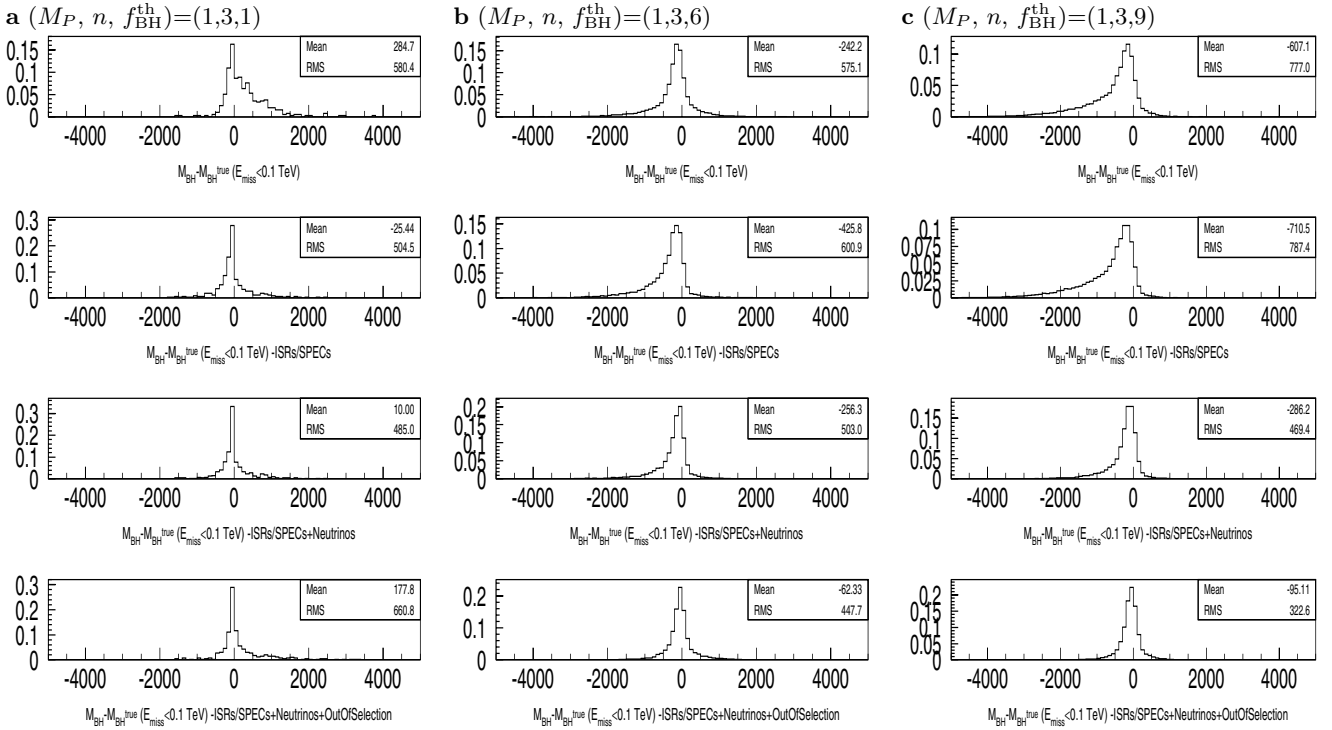
a $(M_P, n, f_{\mathrm{BH}}^{\mathrm{th}}) = (1,3,1)$ **b** $(M_P, n, f_{\mathrm{BH}}^{\mathrm{th}}) = (1,3,6)$ **c** $(M_P, n, f_{\mathrm{BH}}^{\mathrm{th}}) = (1,3,9)$

Fig. 17. $M_{\mathrm{BH}} - M_{\mathrm{BH}}^{\mathrm{true}}$ Distributions. The top figures are the same with Figs. 14. The 2nd, 3rd and bottom figures show $M_{\mathrm{BH}} - M_{\mathrm{BH}}^{\mathrm{true}}$ distributions corrected step-by-step. Details are given in the text

luminosity of 100 pb^{-1} (~ 1 day) if $M_P < 4$ TeV. If we assume validity when $M_{\mathrm{BH}} > M_P + 1$ TeV, the required luminosities are slightly larger.

We also proposed a simple method to estimate the Planck scale M_P. It will be necessary to find a way to estimate the number of large extra dimensions n [13] and to identify the excess as the black holes. The development of more realistic black hole generators is also important for more detailed studies.

Appendix A:
Reconstructed mass of black hole

The resolution in the reconstructed mass of the BH depends on various factors. We investigate reasons for

Table 9. Integrated luminosity (fb^{-1}) required for discovery, for various values of (M_P, n), as a function of $M_{\mathrm{BH}}^{\min}$ ($M_{\mathrm{BH}}^{\min} \geq M_P$). The shaded entry gives the most favorable value in each case of (M_P, n)

(M_P, n)		(1,2)	(3,2)	(4,2)	(5,2)
σ (pb)		9450	25.51	3.738	0.6622
	1.0	1.10×10^{-4}	–	–	–
$M_{\mathrm{BH}}^{\min}$	2.0	1.54×10^{-4}	–	–	–
	3.0	3.97×10^{-4}	1.517×10^{-2}	-	-
(TeV)	4.0	1.3×10^{-3}	3.348×10^{-2}	0.1060	-
	5.0	4.3×10^{-3}	9.43×10^{-2}	0.2472	0.6485

(M_P, n)		(1,3)	(3,3)	(4,3)	(5,3)
σ (pb)		8256	22.89	3.381	0.6027
	1.0	1.43×10^{-4}	–	–	–
$M_{\mathrm{BH}}^{\min}$	2.0	2.07×10^{-4}	–	–	–
	3.0	4.98×10^{-4}	1.701×10^{-2}	–	–
(TeV)	4.0	1.7×10^{-3}	3.643×10^{-2}	0.1233	–
	5.0	8.3×10^{-3}	0.108	0.2822	0.7123

(M_P, n)		(1,5)	(3,5)	(4,5)	(5,5)
σ (pb)		8244	23.42	3.487	0.6252
	1.0	1.68×10^{-4}	–	–	–
$M_{\mathrm{BH}}^{\min}$	2.0	2.36×10^{-4}	–	–	–
	3.0	5.81×10^{-4}	1.786×10^{-2}	–	–
(TeV)	4.0	2.0×10^{-3}	4.005×10^{-2}	0.1121	–
	5.0	7.1×10^{-3}	0.129	0.2650	0.7184

(M_P, n)		(1,7)	(3,7)	(4,7)	(5,7)
σ (pb)		9053	26.02	3.887	0.6991
	1.0	1.69×10^{-4}	–	–	–
$M_{\mathrm{BH}}^{\min}$	2.0	2.37×10^{-4}	–	–	–
	3.0	6.37×10^{-4}	1.585×10^{-2}	–	–
(TeV)	4.0	2.2×10^{-3}	3.586×10^{-2}	0.1060	–
	5.0	2×10^{-2}	0.112	0.262	0.6072

overestimation and underestimation of the reconstructed mass M_{BH} as follows.

Figures 14 show distributions of $M_{\mathrm{BH}} - M_{\mathrm{BH}}^{\mathrm{true}}$ for BH events with $M_{\mathrm{BH}}^{\mathrm{true}} \geq 1.0, 6.0$, and 9.0 TeV in case of $(M_P, n) = (1,3)$, respectively.

There are contaminations from particles arising from the initial state radiation and from the spectator proton fragments of the hard scattering. We call these particles "ISRs/SPECs". Figures 15 show $M_{\mathrm{BH}} - M_{\mathrm{BH}}^{\mathrm{true}}$ distributions of the events with no neutrino. We compare the difference in mass when all particles are used and when ISRs/SPECs are excluded. The generator information is used to determine whether a particle comes from ISRs/SPECs. We can see that the overestimation of a black hole mass is due to the contaminations of ISRs/SPECs.

Figure 16 shows the correlation between a $M_{\mathrm{BH}} - M_{\mathrm{BH}}^{\mathrm{true}}$ and a measured missing energy $\not{E}_T$. We can see clearly that we underestimate a black hole mass if the missing energy is important.

We perform various corrections:(1) we subtract the momentum of particles which are selected by our criteria but come from ISRs/SPECs, from the reconstructed mass M_{BH}, (2) add the momentum of neutrinos, (3) add the momentum of particles which do not come from ISRs/SPECs but are removed by our selection criteria, as shown at Figs. 17. We can see that the reconstructed mass is improved by these corrections as we expected. From these results we understand that the overestimation of M_{BH} is caused by the contamination of particles from the initial state radiation and the spectators while the underestimation is due to the missing energy of neutrinos.

References

1. S. Dimopoulous, G. Landsberg, Phys. Rev. Lett. **87**, 161602 (2001)
2. S. B. Giddings, S. Thomas, Phys. Rev. D **65**, 056010 (2002)
3. N. Arkani-Hamed, S. Dimopoulous, G. Dvali, Phys. Lett. B **429**, 263 (1998)
4. J. Chiaverini, S.J. Smullin, A.A. Geraci, D.M. Weld, A. Kapitulnik, Phys. Rev. Lett. **90**, 151101 (2003)
5. Particle Data Group, K. Hagiwara et al., Phys. Rev. D **66**, 010001 (2002)
6. Y. Uehara, Mod. Phys. Lett. A **17** 1551 (2002)
7. M.B. Voloshin, Phys. Lett. B **518**, 137 (2001); M.B. Voloshin Phys. Lett. B **524**, 376 (2002)
8. D.M. Eardley, S.B. Giddings, Phys. Rev. D **66**, 044011 (2002); H. Yoshino, Y. Nambu, Phys. Rev. D **66**, 065004 (2002); H. Yoshino, Y. Nambu, Phys. Rev. D 67, 024009 (2003); S.N. Solodukhin, Phys. Lett. B **533**, 153 (2002); S.D.H. Hsu Phys. Lett. B **555**, 92 (2003)
9. T. Sjostrand et al., hep-ph/018264. PYTHIA 6.206 is used for the signal and 6.203 for the background
10. E. Richter-Was, D. Froidevaux, L. Poggioli, ATLAS internal note ATL-PHYS-98-131 (1998)
11. G. Landsberg, SUSY 2002 Conference, DESY, Hamburg, June 17–23, 2002, hep-ph/0211043
12. The other black hole generator, CHARYBDIS, has been developed, which takes into account more realistic effects. See C. M. Harris, P. Richardson, B. R. Webber, JHEP **0308**, 033 (2003)
13. C. M. Harris et al., hep-ph/0411022